

New route for stabilization of 1T-WS₂ and MoS₂ phases

Andrey N. Enyashin,^{*a,b} Lena Yadgarov,^c Lothar Houben,^d Igor Popov,^e Marc Weidenbach,^d Reshef Tenne,^c Maya Bar-Sadan^{*d}, and Gotthard Seifert^a

5 The phenomenon of a partial 2H→1T phase transition within multiwalled WS₂ nanotubes under substitutional Rhenium doping is discovered by means of high-resolution transmission electron microscopy. Using density-functional calculations for the related MoS₂ compound we consider a possible origin of this phase transition, which was known formerly only for WS₂ and MoS₂ intercalated by alkali metals. An interplay between the stability of layered or nanotubular forms of 2H and 1T allotropes is
10 found to be intimately related with their electronic structures and electro-donating ability of an impurity.

1. Introduction

Co-generic molybdenum and tungsten disulfides (MS₂, M = Mo, W) are typical representative compounds of the rather extensive family of layered chalcogenides. Their metal atoms have a six-
15 fold coordination environment and are hexagonally packed between two trigonal atomic layers of S atoms. Depending on the arrangement of the S atoms two kinds of the hexagonal S-M-S triple layers are possible, which are composed by either prismatic D_{3h}- or octahedral O_h-MS₆ units (Fig. 1). Such triple layers
20 interact by weak van-der-Waals interactions and may be stacked in different ways. For example, natural MoS₂ occurs as a mixture of two stable polymorphs based on D_{3h}-MoS₆ units: the hexagonal 2H-MoS₂ and the rhombohedral modification 3R-MoS₂, which unit cells include two and three S-M-S monolayers,
25 respectively [1]. The 2H-polytype is dominant and more stable, hence the 3R-polytype transforms into the first one upon heating. Further polytypic structures, other than 2H or 3R, have been predicted [2], but have not yet been observed experimentally.

A MS₂ polytype based on O_h-MS₆ units has not been found in
30 the nature and it is recognized as unstable [1]. Nevertheless, S-M-S layers with an octahedral coordination of metal atoms can be synthesized under intercalation of a 2H-MS₂ host lattice by alkali-metals Li and K, forming 1T-Li_xMS₂ and 1T-K_xMS₂ phases [3-5]. Moreover, subsequent solvation and reduction of
35 these intercalates leads to the exfoliation and release of free 1T-MS₂ layers [5-8]. Depending on the composition of the intercalate, reducing agent used and temperature, the monolayers of 1T-MoS₂ and 1T-WS₂ can restack to form various superstructures as revealed by Raman-scattering [9], electron and
40 x-ray diffraction [9-11] and scanning tunneling microscopy [12]. However, these metastable materials undergo an irreversible transition to 2H-MS₂ phases already at 95 °C [5]. Theoretical considerations of the interlayer S/S and intra-layer M/S glide within MoS₂ crystals clearly explained the preference of the 2H-
45 MoS₂ allotrope over the 1T-MoS₂ structure [13].

Nowadays, micro- and nanosized particles of 2H-MoS₂ and 2H-WS₂ play a major role in the catalytic refinement of petroleum oils [14]. Numerous quantum-mechanical calculations reveal a correlation between their catalytic activity and metallic

50 character of their edges [15-17], while the bulk crystals of these compounds are semiconductors [18,19]. Interestingly, quantum-mechanical calculations for the band structure of the unstable 1T-MoS₂ suggest that the ground state of this system is metallic and consequently it may possess high catalytic activity [20,21].
55 Thereby, there is an interest to search for a possible way of stabilizing the 1T-MoS₂ and 1T-WS₂ phases. Recently, significant progress has been achieved in doping MoS₂ and WS₂ closed-cage structures by Re [22], rendering the structures superior lubricating properties.

60 In this work we report the discovery of 1T-MS₂ phase within WS₂ nanotubes substitutionally doped by Rhenium. Such doped and still covalently bound lattice of the 1T-phase should be genuinely more stable comparing with the lattice of alkali-intercalated compound. Using quantum-mechanical calculations
65 for the related MoS₂ compound we consider a possible origin of this phase and its stability in layered and nanotubular states, which are found to be intimately related with the electronic structures of 2H- and 1T-MS₂ allotropes and electro-donating character of Re impurities. Finally, we hypothesize about high
70 catalytic and tribologic characteristics of these doped nanotubes and fullerene-like particles.

2. Methods

2.1. Synthesis of Re (~2 at%) doped WS₂ nanotubes

ReO₃ was added to a vertical quartz ampoule at its “hot” zone
75 (bottom of the ampoule) containing inorganic WS₂ nanotubes at the “cold” zone (middle of the ampoule) and I₂ (~80 mg), which later serves as carrier agent (see Fig. 1). The ampoule was cooled with liquid nitrogen, evacuated to ~10⁻⁵ Torr and sealed. The distance between the hot and the cold zone was ~12 cm, long
80 enough to avoid excess doping. The ampoule was placed in a two-zone furnace and allowed to react for 22 hours at 800⁰C (cold zone) to 950⁰C (hot zone). The temperature gradient is intended to prevent back transport of the product. Afterwards the ampoule was quenched in order to stop the reaction at once. The
85 rhenium composition *x* was estimated by EDS (energy dispersive X-ray spectroscopy), and analyzed by SEM (scanning electron microscopy) and TEM (transmission electron microscope).

2.2. Microscopy Methods

Electron microscopy images were taken with an image-side aberration-corrected FEI Titan 80-300 transmission electron microscope operated at 300 kV. Negative spherical aberration imaging (NCSI) conditions were applied [23,24]. These conditions produce high sensitivity even for light elements and yield images that are a close representation of the projected potential for sufficiently thin samples, meaning that the image intensity can be correlated with the location of the atoms Phase retrieval from focal series was employed to enhance the signal-to-noise ratio and to eliminate the effect of residual aberrations [25].

Image simulations for NCSI conditions were done using model nanostructures with multislice calculations, to confirm the coordination between Mo and S atoms. Special care was taken to ensure, that both pattern and spatial distances match the models unequivocally, since different projections and tilts of the model might yield similar patterns.

2.3. Models and Computational Methods

Supercells of MoS₂ monolayers, double layers, single- and double-walled nanotubes were chosen as the models for the study of pure and doped 1T- and 2H-allotropes. MoS₂ monolayer and double layer supercells were composed of 10x10x1 and 5x5x2 MoS₂ unit cells, respectively. The models of MoS₂ nanotubes were represented with combinations of supercells for (14,14) and (21,21) nanotubes each composed of 7 elementary unit cells. The classification and construction principles of single-walled MoS₂ nanotubes was reported earlier [26].

All of the stability and electronic structure calculations with full geometry optimization and molecular dynamic simulations were performed with the density-functional-based tight-binding (DFTB) method [27,28], which formerly was applied in numerous studies of MoS₂ nanostructures [26,29,30].

3. Results and Discussion

3.1. Microscopy data

The direct observation by electron microscopy of Re atoms within the lattice of MoS₂ or WS₂ is practically impossible because of several reasons: the doping level of the nanotubes is very low (<1%) and the doping is homogeneous, therefore, the Re atoms do not produce much disorder within the lattice. The atomic number of Re is close to Mo and much smaller than W, therefore it does not create significant change of contrast in the images. The low doping level also hinders the use of electron energy loss spectroscopy (EELS) to detect the existence and place of the single Re atoms. However, EXAFS experimental results confirm the existence of individual atoms of Re as well as very small clusters of them within the lattice [22].

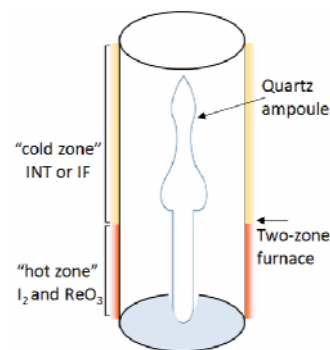


Fig. 1. Schematic drawing of the experimental setup: the reactants (WS₂ nanotubes, ReO₃ and I₂) are put within an evacuated quartz ampoule placed inside a two-zone furnace.

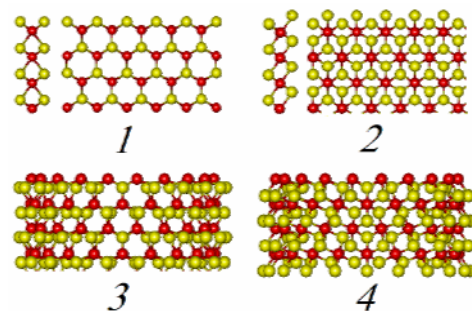


Fig. 2. Monolayers of 2H- (1) and 1T- (2) allotropes of transition metal sulfides MS₂ (M = W, Mo) composed of prismatic or octahedral units MS₆, respectively (the side and the top views are depicted). Below the models of single-walled zigzag (20,0) nanotubes are shown for 2H- (3) and 1T- (4) (lateral view).

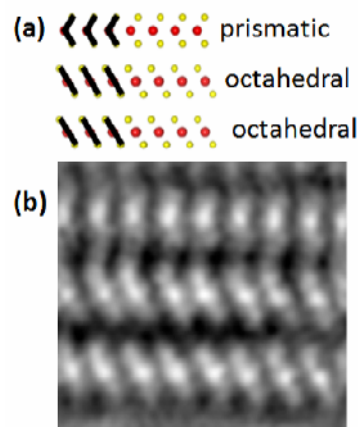


Fig. 3. A schematic representation of the octahedral and the prismatic polytypes of MoS₂/WS₂ (a). The prismatic layer is imaged as a chevron pattern, while the octahedral one creates a diagonal pattern. Mo/W in red, S in yellow. (b) Wavefunction reconstructed from a focal series taken at 300 kV, showing the outermost walls of Re-doped WS₂ nanotubes. As it is presented in (a), the two outermost layers are octahedral and the inner one is prismatic.

The different structural phases of WS₂ are directly distinguishable by HRTEM. The prismatic coordination of the S-M-S creates a chevron pattern, while the octahedral one is imaged as a diagonal line (See Fig. 3a) [30]. In the nanotubes presented, two layers of 1T-phase with octahedral coordination of metal atoms are seen at the outermost shells, followed by a prismatic inner layer of 2H-phase (see Fig. 3b). The observation of a few

dozens of nanotubes showed a dominance of prismatic D_{3h} - MS_6 coordination while patches of single octahedrally coordinated layers can be found at or close to the nanotube surface at 10% of the structures..

In further, we employ the density-functional calculations in order to explain the occurrence of unstable 1T- MS_2 phase.

3.2. Stability of undoped 1T-MoS₂ nanotubes

The results of DFTB calculations for the stability of pure 1T-MoS₂ single-walled nanotubes are shown in Fig. 4. It can be seen, that the curve of strain energy (E_{str}) versus radius, relative to the monolayer, shows similar trends in analogy to many other compounds, e.g. carbon and 2H-MoS₂ [26,31]. The strain energy is inversely proportional to the radius R as $E_{str} = a/R^2$ and is also nearly independent of the chirality type. At the same time, the energies indicate a much lower stability of 1T-MoS₂ nanotubes comparing to the nanotubes based on the 2H-MoS₂ allotrope due to both the higher energy of 1T-monolayer on 0.27 eV/atom and a slightly larger strain energy factor $a = 18.6 \text{ eV}\cdot\text{\AA}^2/\text{atom}$ versus $15.8 \text{ eV}\cdot\text{\AA}^2/\text{atom}$ for 2H-MoS₂ nanotubes.

The calculated high energies of 1T-MoS₂ nanotubes might hint that the much more stable inner core of 2H-WS₂ nanotubes stabilizes the 1T-WS₂ phase observed in the HRTEM of multiwalled sulfide nanotubes. In order to prove this idea, additional molecular dynamics simulations of double-walled MoS₂ nanotubes composed by single-walled nanotubes of 1T- and 2H-MoS₂ modifications with all possible mutual arrangements were performed (Fig. 5). However, according to the calculations, double-walled nanotubes containing at least one shell of 1T-MoS₂ phase undergo essential distortions or even disintegrate into a bundle of nanostripes. Thus, it is likely that the formation of the unfavorable 1T-phase within a multiwalled sulfide nanotubes is enhanced by the influence of Re in Re-doped MS₂ nanotubes.

Calculated densities-of-states (DOS) for some selected 1T- and 2H-MoS₂ nanostructures are drawn on Fig. 6. In both cases of allotropes there is no essential difference in the DOS profiles between the nanotubes of different chiralities and for the corresponding bulk and monolayer.

In the calculated electronic structure of the most stable 2H-MoS₂ allotrope three bands can be clearly distinguished, which agrees with the results of former experimental and quantum-mechanical investigations [19]. The valence band composed mainly of the $S3p$ -states is separated from the Fermi level by ~ 3.5 eV. The states below and near the Fermi level are Mo $4d$ -states. The bottom of the conduction band is also composed of Mo $4d$ -states. Therefore, 2H-MoS₂ is a semiconductor with a band gap around 1.2 – 1.3 eV, which in the case of nanotubes may be slightly smaller depending on their radii [26]. In the framework of crystal field theory the semiconducting nature of 2H-MoS₂ is caused by the symmetry-induced splitting of the Mo $4d$ -orbitals of a D_{3h} -MoS₆ unit into three groups: (1) Mo $4d_{z^2}$, which is completely occupied, (2) Mo $4d_{xy}$ and Mo $4d_{x^2-y^2}$ and (3) Mo $4d_{xz}$ and Mo $4d_{yz}$, which are unoccupied (Fig. 6).

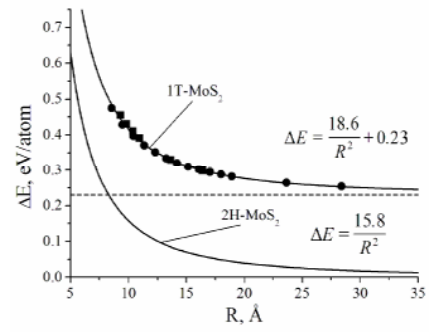


Fig. 4. The energies ΔE of 1T-MoS₂ monolayer (dashed line) and 1T-MoS₂ based single-walled nanotubes (■ – zigzag and ● – armchair chiralities) relative to the energy of 2H-MoS₂ based monolayer. For comparison the energies of 2H-MoS₂ single-walled nanotubes are also depicted (adapted from [26]).

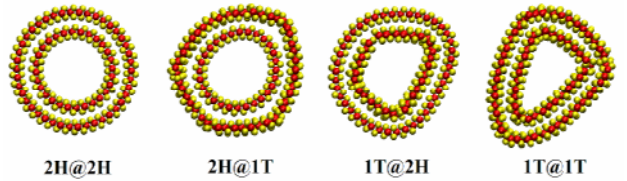


Fig. 5. Final MD snapshots ($T = 300 \text{ K}$) for double-walled (14,14)@(21,21)MoS₂ nanotubes composed by the single-walled nanotubes of different allotropes: the layers with prismatic (like in 2H-phase) and octahedral (like in 1T-phase) coordination of metal atoms. All nanotubes containing 1T modification are unstable and decompose partially or totally into a bundle of nanostripes.

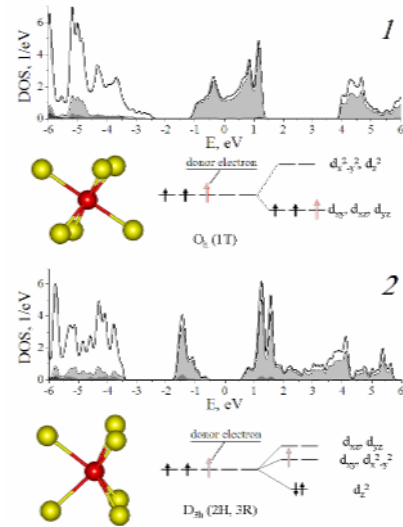


Fig. 6. Total (full line) and partial Mo $4d$ densities of states (DOS) for (14,14) 1T-MoS₂ (1) and - (14,14) 2H-MoS₂ nanotubes (2) and their simplified representations within crystal field theory. Mo $4d$ -states are painted in gray. Fermi level is set to 0.0 eV. An electron donating of Mo d_{xy} levels can stabilize 1T-MoS₂ phase and destabilize 2H-MoS₂ phase.

Both the monolayer and the nanotubes of 1T-MoS₂ allotrope show metal-like character (see Fig. 6). It agrees with the results of previous calculations and experimental data [20,21]. Like in the case of 2H-MoS₂ the valence band of the $S3p$ -states is separated from the Fermi level by ~ 3 eV. Though, the Mo $4d$ -states in 1T-MoS₂ form a single wide band, which hosts the Fermi level. In terms of crystal field theory the origin of the latter

band can be described as splitting of the $Mo4d$ -orbitals of a O_h - MoS_6 unit into two groups: (1) three degenerated $Mo4d_{xy,yz,xz}$ -orbitals populated only by two electrons, and (2) non-occupied $Mo4d_{z^2}$ and $Mo4d_{x^2-y^2}$ levels (Fig. 6).

The incomplete occupation of $Mo4d_{xy,yz,xz}$ -orbitals in 1T- MoS_2 leads to the metallic ground state but it also decreases the stability of this MoS_2 allotrope. Therefore, by doping the 1T- MoS_2 lattice with a donor atom, the additional electrons occupy the $Mo4d_{xy,yz,xz}$ -orbitals and increase the stability of the 1T phase. On the contrary, when such doping occurs in the semiconducting 2H- MoS_2 allotrope, the electrons which are donated to the $Mo4d_{xy,yz,xz}$ orbitals and to the $Mo4d_{x^2-y^2}$ orbitals result in the metallic-like character of the electronic structure and it causes destabilization of the lattice. Similar analysis of the population of $Mo4d$ -orbitals in both MoS_2 allotropes can explain the transition from 2H- MS_2 lattice to 1T- MS_2 lattice in MoS_2 and WS_2 when intercalated by the electron-donating atoms of alkali-metals [5-7]. Moreover, it suggests that a similar transition and appearance of the 1T-phase may happen as a result of substitutional doping by atoms of d -elements which can serve as electron donors. For example, atoms such as Re, Tc, Mn, which have more valence electrons, than Mo or W may act as donors. Our further DFTB calculations for various polytypes of MoS_2 doped with different amount of Re atoms support this assumption.

3.3. Relative stability of 1T-, 2H- and mixed (1T,2H)- $Mo_{1-x}Re_xS_2$ allotropes

As the first step the study of the substitution of Mo atoms by Re atoms within 1T- and 2H- MoS_2 polytypes was performed by varying the Re content (x) and the arrangement of doping atoms. The consideration of low Re concentrations requires the use of supercells of corresponding single- and multi-walled MoS_2 nanotubes, which would contain a too large number of atoms. There are also too many possible variants of substitutions for the Re atoms. Thus, in further study we have focused our attention on a more simple case of single and double layers. As the most limiting variants of rhenium distribution, two variants were taken into account: when the Re atoms segregate to make an island of ReS_2 phase embedded within the MoS_2 lattice and when the Re atoms are scattered randomly within the sublattice of the metal atoms. The relative stability of any doped $Mo_{1-x}Re_xS_2$ ($x = 0.0 \dots 1.0$) monolayer was characterized as the energy difference ΔE compared to the 2H- $Mo_{1-x}Re_xS_2$ monolayer with random distribution of Re atoms.

The calculated values of ΔE are plotted in Fig. 7. An island-like substitutional Re doping is slightly more favored than a random distribution of Re atoms over a wide range of x , for both kinds of MoS_2 polytypes. Nevertheless, the maximal energy difference due to the various arrangement of Re atoms at any Re content does not exceed 0.02 eV/atom, which is much smaller relative to the energy differences between the different polytypes. It can be seen that all 1T- $Mo_{1-x}Re_xS_2$ phases are still clearly higher in energy, than their corresponding 2H- $Mo_{1-x}Re_xS_2$ phases (Fig. 7). However, the doping may essentially change the energy difference (ΔE) between 1T- and 2H-phase. While for pure MoS_2 phases ΔE is 0.23 eV/atom, it decreases at higher x and adopts its minimal value at $x = 0.6$, which is only 0.03 eV/atom.

Thus, the calculations show, that the competitive existence of 1T- $Mo_{1-x}Re_xS_2$ phase could be achieved in practice at a finite

temperature and high Re concentration, when the impurity atoms donate the electrons to the Mo sublattice of hosting MoS_2 monolayer. However, for the case of a multilayered crystal or multiwalled nanotube a question may appear, if the donor electrons can be adopted from the Re atoms hosted in a neighboring MoS_2 layer?

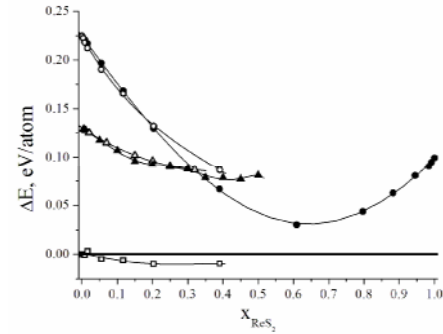


Fig. 7. Relative energies of $Mo_{1-x}Re_xS_2$ layers depending on the Re content. All energies are given relative to 2H- $Mo_{1-x}Re_xS_2$ monolayer with random Re distribution. \square – energies of 2H- $Mo_{1-x}Re_xS_2$ monolayer with “cluster” of Re atoms, \bullet – energies of 1T- $Mo_{1-x}Re_xS_2$ monolayer with random Re distribution, \circ – energies of 1T- $Mo_{1-x}Re_xS_2$ monolayer with “cluster” of Re atoms, \blacktriangle – energies of mixed (1T- MoS_2 , 2H- $Mo_{1-x}Re_xS_2$) bilayer with random Re distribution, Δ – energies of (1T- MoS_2 , 2H- $Mo_{1-x}Re_xS_2$) bilayer with “cluster” of Re atoms.

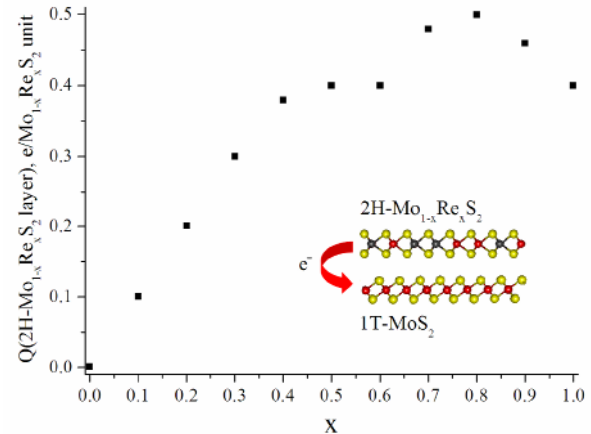


Fig. 8. Charge of 2H- $Mo_{1-x}Re_xS_2$ layer within (1T- MoS_2 , 2H- $Mo_{1-x}Re_xS_2$) bilayer as function of the Re content

To examine this problem similar energy calculations were performed on a MoS_2 bilayer composed of adjacent 1T- MoS_2 and 2H- $Mo_{1-x}Re_xS_2$ monolayers (Fig. 7). As it was expected, the relative energy of such mixed (1T,2H)-allotrope for undoped MoS_2 is almost the average between the energies of separated 1T- and 2H- MoS_2 allotropes. A small deviation from the ideal ΔE value can be explained by the limitations of the model in describing the superstructure of (1T,2H)- MoS_2 composed of two slightly mismatched lattices of 1T- and 2H- MoS_2 monolayers. Under doping of the 2H- MoS_2 layer, the relative energy ΔE of mixed (1T- MoS_2 , 2H- $Mo_{1-x}Re_xS_2$)-bilayer decreases with increasing of Re content, and it is lower than the ΔE for the simple 1T- $Mo_{1-x}Re_xS_2$ allotrope until the doping content reaches $x=0.35$. Noticeably, this correlation between ΔE for different variants of Re distribution points out that in the mixed and doped (1T,2H)-allotrope the Re atoms should play the same role of the

electron donors as in the 1T-Mo_{1-x}Re_xS₂ phase. An analysis of the charge distribution supports this guess (Fig. 8). For a (1T-MoS₂, 2H-Mo_{1-x}Re_xS₂)-bilayer an almost linear increase of an electron transfer from the Re-doped layer to the pure MoS₂ layer can be seen until $x \approx 0.4$.

4. Conclusions

Our work evidences that the occurrence of a 1T-phase revealed by HRTEM methods within disulfide WS₂ nanotubes should be stimulated using substitutional doping of Re atoms, which destabilizes the 2H-phase. The Re impurity atoms within the lattice of WS₂ or related MoS₂ serve as electron-donors, when they are placed within the same layer of the 1T-allotrope as well as placed in the neighboring layer of the 2H-allotrope. Due to equal energy costs, there is no essential preference among both these variants. The distribution of Re atoms within a multiwalled sulfide nanotube should be determined by the fabrication route. For example, in nanotubes fabricated using the gas-phase sulfurization of a mixture of volatile Re and W or Mo chlorides [32], where the reactants themselves already contain Re atoms, Re atoms may be distributed within all the volume of the walls. In contrast, treatment of the already prepared MoS₂ or WS₂ sulfide nanotubes in the vapor of Re halides (as in the current work) might induce the diffusion of Re atoms only into the lattice of the surface layers.

MoS₂ and WS₂ are one of the most exploited compounds among transition metal sulfides, which play a major role in the catalytic refinement of petroleum oils and are the main components of technical lubricants in aerospace industry [14,33]. The results of our calculations indicate that Re doping of these nanostructured sulfides could be important in an improvement of both technological applications. It is revealed that the formation of 1T-allotrope as the outer layers of sulfide nanotubes may be induced by the electron-donation from the neighboring doped layers of 2H-phase. This charge transfer reflects the rise of a surface dipole, which points along the normals of layers. Such an enlarged electronic density on the outer walls of a nanotube can be associated with their higher reactivity. This finding opens up a perspective for the Re-doped WS₂ and MoS₂ nanotubes as superior catalysts similar to the sulfide nanoplatelets [14,17,30].

Numerous former experiments have demonstrated that the quasi-spherical or tubular morphology of 2H-WS₂ or 2H-MoS₂ nanoparticles, provides a lower density of dangling bonds in comparison to simply nanosized particles of the bulk material and allows a significant increase of the tribological and anti-wear characteristics [33]. The calculations have shown that the strain-stress relationship of the multi-walled sulfide particles is determined by the smallest, innermost wall [34]. Under a load during wear the particles are being broken from the inside to the outside until a bundle of the nanostripes occurs, which are always parallel to the working surfaces and form nanocoating [34]. Obviously even these superior tribological characteristics of MoS₂ and WS₂ fullerene-like particles and nanotubes can be improved further using Re doping. The present calculations reveal a higher (comparing with 2H-MoS₂) strain and, following, a lower mechanical resistance of 1T-MoS₂ shells. When the 1T phase occurs at the outer surface of doped multiwalled sulfide nanotubes, a lower wear coefficient can be achieved due to the

more premature break and exfoliation of the outer shells. These may serve later, after the adhesion on the working surfaces, as a smear undercoat for the rest of the multiwalled particles, and provides the better bearing effect. Further experimental as well as theoretical studies should verify these preliminary suggestions.

Acknowledgments

The support of the ERC project INTIF 226639 is gratefully acknowledged. A.E. thanks grant RFBR 11-03-00156-a.

Notes

^a Physical Chemistry Department, Technical University Dresden, Bergstr. 66b, 01062 Dresden, Germany. Fax: +49 (0) 351 463 35953; Tel: (+49) (351) 463 37637; E-mail: enyashin@ihim.urban.ru;

⁷⁰ gotthard.seifert@chemie.tu-dresden.de

^b Institute of Solid State Chemistry UB RAS, Pervomayskaya Str. 91, 620990 Ekaterinburg, Russia. Fax: +7 343 374 4495; E-mail: enyashin@ihim.urban.ru

⁷⁵ Materials and Interfaces Departament, Weizmann Institute of Science, 76100 Rehovot, Israel. E-mail: reshef.tenne@weizmann.ac.il

^d Peter Grünberg Institute, Ernst Ruska-Centre for Microscopy and Spectroscopy with Electrons, Research Centre Juelich, 52425 Juelich, Germany. Fax: +49 (0) 246 161 6444; E-mail: m.bar-sadan@fz-juelich.de; l.houben@fz-juelich.de

⁸⁰ School of Physics and CRANN, Trinity College, Dublin 2, Ireland.

References

- 1 H. Bergmann, B. Czeska, I. Haas, B. Mohsin and K.-H. Wandner, *Gmelin Handbook of Inorganic and Organometallic Chemistry*, Vol. B7 (Springer-Verlag, Berlin, 1992)
- 85 2 B.B. Zvyagin and S.V. Soboleva, *Sov. Phys. Crystallogr.*, 1967, **12**, 46.
- 3 M.A. Py and R.R. Haering, *Can. J. Phys.*, 1983, **61**, 76.
- 4 N. Imanishi, M. Toyoda, Y. Takeda and O. Yamamoto, *Solid State Ionics*, 1992, **58**, 333.
- 90 5 F. Wypych and R. Schöllhorn, *J. Chem. Soc. Chem. Commun.*, 1992, 1386.
- 6 D. Yang and R.F. Frindt, *J. Phys. Chem. Solids*, 1996, **57**, 1113.
- 7 R.A. Gordon, D. Yang, E.D. Crozier, D.T. Jiang and R.F. Frindt, *Phys. Rev. B*, 2002, **65**, 125407.
- 95 8 H.-L. Tsai, J. Heising, J.L. Schindler, C.R. Kannewurf and M.G. Kanatzidis, *Chem. Mater.*, 1997, **9**, 879.
- 9 D. Yang, S. Jiménez, W.M.R. Divigalpitiya, J.C. Irwin and R.F. Frindt, *Phys. Rev. B*, 1991, **43**, 12053.
- 10 F. Wypych, C. Solenthaler, R. Prins and T. Weber, *J. Solid State Chem.*, 1999, **144**, 430.
- 100 11 J. Heising and M.G. Kanatzidis, *J. Am. Chem. Soc.*, 1999, **121**, 638.
- 12 F. Wypych, T. Weber and R. Prins, *Chem. Mater.*, 1998, **10**, 723.
- 13 Y. Rosenfeld Hachon, R. Popovitz-Biro, Y. Prior, S. Gemming, G. Seifert and R. Tenne, *Phys. Chem. Chem. Phys.*, 2003, **5**, 1644.
- 105 14 R.R. Chianelli, M.H. Siadati and M.P. De la Rosa, *Catalysis Rev.*, 2006, **48**, 1.
- 15 S. Helveg, J.V. Lauritsen, E. Lagsgaard, I. Stensgaard, J.K. Nørskov, B.S. Clausen, H. Topsøe and F. Besenbacher, *Phys. Rev. Lett.*, 2000, **84**, 951.
- 110 16 J. Kibsgaard, J.V. Lauritsen, E. Lagsgaard, B.S. Clausen, H. Topsøe and F. Besenbacher, *J. Am. Chem. Soc.*, 2006, **128**, 13950.
- 17 J.V. Lauritsen, J. Kibsgaard, S. Helveg, H. Topsøe, B.S. Clausen, E. Lagsgaard and F. Besenbacher, *Nature Nanotech.*, 2007, **2**, 53.
- 18 A. Klein, S. Tiefenbacher, V. Eyert, C. Pettenkofer and W. Jagermann, *Phys. Rev. B*, 2001, **64**, 205416.
- 115 19 T. Böker, R. Severin, A. Müller, C. Janowitz, R. Manzke, D. Voß, P. Krüger, A. Mazur and J. Pollman, *Phys. Rev. B*, 2001, **64**, 235305.
- 20 K.E. Dungey, M.D. Curtis and J.E. Penner-Hahn, *Chem. Mater.*, 1998, **10**, 2151.

-
- 21 V. Alexiev, R. Prins and T. Weber, *Phys. Chem. Chem. Phys.*, 2000, **2**, 1815.
- 22 L. Yadgarov, R. Rosentsveig, G. Leitun, A. Albu-Yaron, A. Moshkovich, V. Perilyev, R. Vasic, A. I. Frenkel, A. N. Enyashin, G. Seifert, L. Rapoport and R. Tenne, *Submitted*.
- 5 23 C.L. Jia and K. Urban, *Science*, 2004, **303**, 2001.
- 24 M. Lentzen, *Microscopy and Microanalysis*, 2006, **12**, 191.
- 25 K. Tillmann, A. Thust and K. Urban, *Microscopy and Microanalysis*, 2004, **10**, 185.
- 10 26 G. Seifert, H. Terrones, M. Terrones, G. Jungnickel and T. Frauenheim, *Phys. Rev. Lett.*, 2000, **85**, 146.
- 27 G. Seifert, D. Porezag and T. Frauenheim, *Intern. J. Quant. Chem.*, 1996, **58**, 185.
- 28 L. Zhechkov, T. Heine, S. Patchkovskii, G. Seifert and H.A. Duarte, *J. Chem. Theory and Computation*, 2005, **1**, 841.
- 15 29 A.N. Enyashin, S. Gemming, M. Bar-Sadan, R. Popovitz-Biro, S.Y. Hong, Y. Prior, R. Tenne and G. Seifert, *Angew. Chem. Int. Ed.*, 2007, **46**, 623.
- 30 A.N. Enyashin, M. Bar-Sadan, J. Sloan, L. Houben and G. Seifert, *Chem. Mater.*, 2009, **21**, 5627.
- 20 31 R. Tenne, M. Remškar, A.N. Enyashin and G. Seifert, *Topics Appl. Phys.*, 2008, **111**, 631.
- 32 F.L. Deepak, R. Popovitz-Biro, Y. Feldman, H. Cohen, A.N. Enyashin, G. Seifert and R. Tenne, *Chem. Asian J.*, 2008, **3**, 1568.
- 25 33 R. Tenne and M. Redlich, *Chem. Soc. Rev.*, 2010, **39**, 1423.
- 34 M. Stefanov, A.N. Enyashin, T. Heine and G. Seifert, *J. Phys. Chem. C*, 2008, **112**, 17764.